Supplementary figure 1

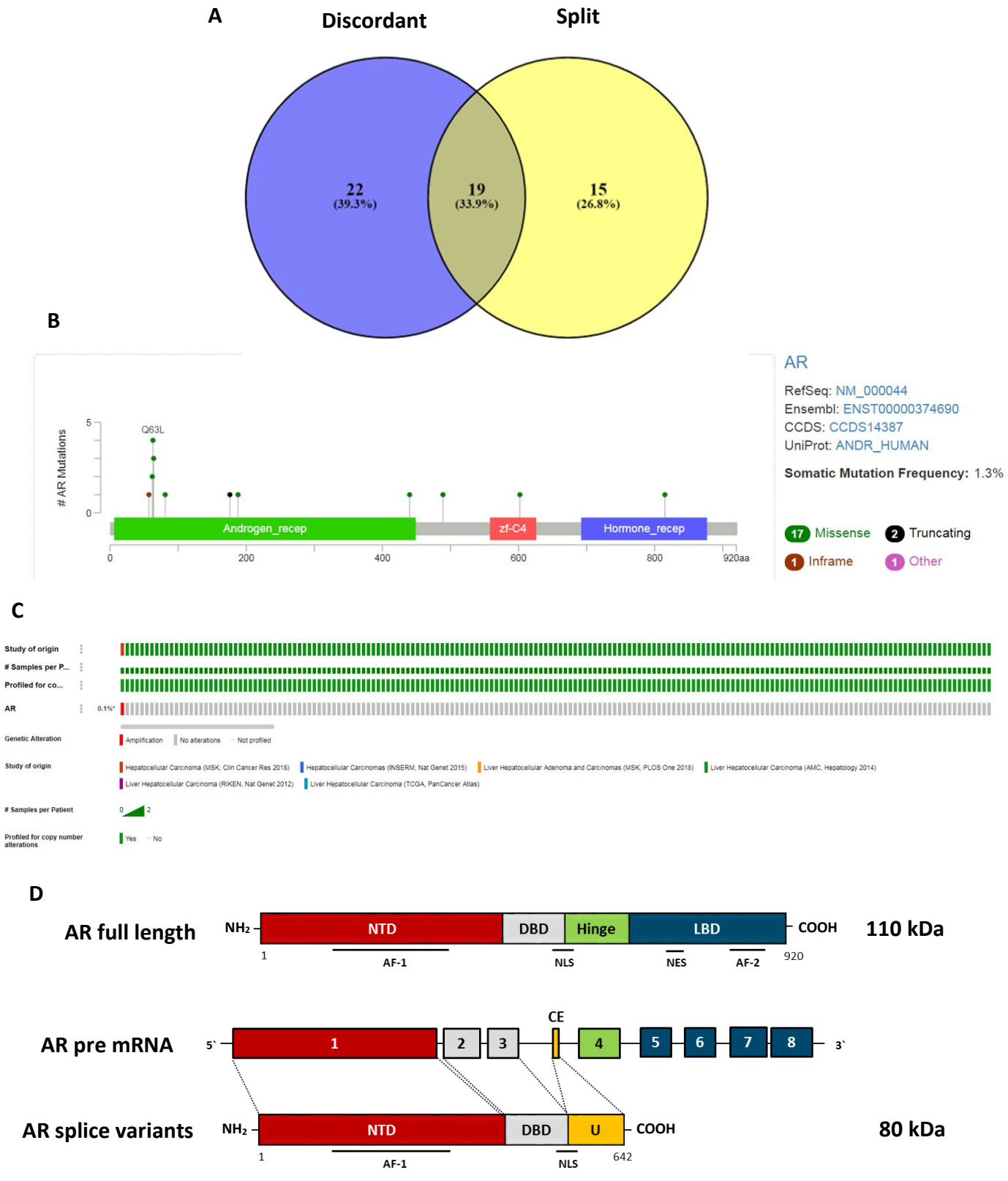

Supplementary Figure 1. Potential mechanisms for antiandrogen resistance in HCC and Survey of AR gene alterations in publicly available primary HCC samples. (a) Read pairs supporting the deletion of exons 4-8 of the AR gene in SNU-475 and were classified as discordant (R1 and R2 mapping to opposite sides of the deletion) or split reads (reads with partial sequences aligning on each side of the deletion). 19 of the read pairs had both discordant alignments and split read sequences providing strong short read sequencing support for the presence of the deletion. (b) Mutations in the AR gene were surveyed in multiple HCC cohorts (1019 samples) as indicated in the materials and methods section. Specific mutations and their locations are noted. (c) The displayed OncoPrint tab summarizes the absence of AR genomic copy number alterations across all HCC primary samples queried. (d) Schema representing alternative splicing of AR pre-mRNA. AR pre-mRNA is spliced into AR full length which incorporates 8 conical exons that encode for 3 functional domains, NTD, DBD and LBD, and the hinge region. Alternatively, AR pre-mRNA is spliced into C-terminal truncated AR isoforms that incorporate cryptic exons (CE). These cryptic exons carry premature stop codon which results in truncated transcripts that lack the LBD.

Supplementary figure 2

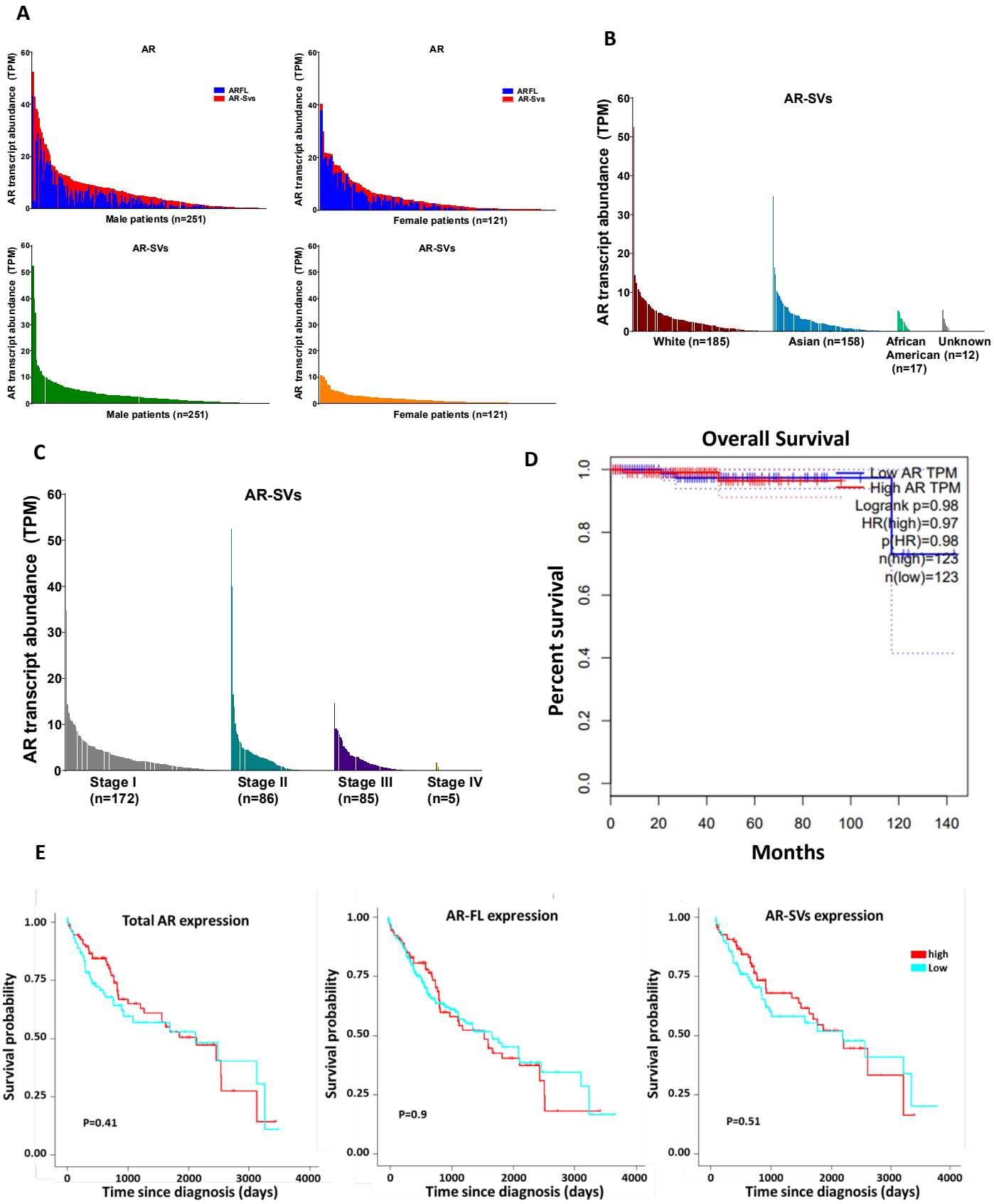

Supplementary Figure 2. Clinical significance of AR signaling in HCC. (a) RNA-Seq data from TCGA LIHC cohort were interrogated for AR transcript expression in female (n=121) and male (n=251) patients. The upper panels show total AR expression partitioned into AR-FL (blue) and AR-Svs (red). Whereas the lower panels compare AR-SVs transcript expression between male and female. (b) RNA-Seq data from TCGA LIHC cohort were interrogated for AR transcript expression based on self-reported race. (c) AR-SVs expression in Caucasian and Asian patients were stratified based on the pathological stage of HCC.(d) Kaplan-Meier survival curves were generated with total AR mRNA from TCGA prostate cancer cohort . (e) Kaplan-Meier survival curves were generated with total AR mRNA (*left*), AR-FL mRNA (*middle*) and AR-SVs mRNA (*right*) from TCGA HCC cohort . Red and turquoise lines represent high and low mRNA expression, respectively. No differences in overall survival were apparent.

Supplementary figure 3

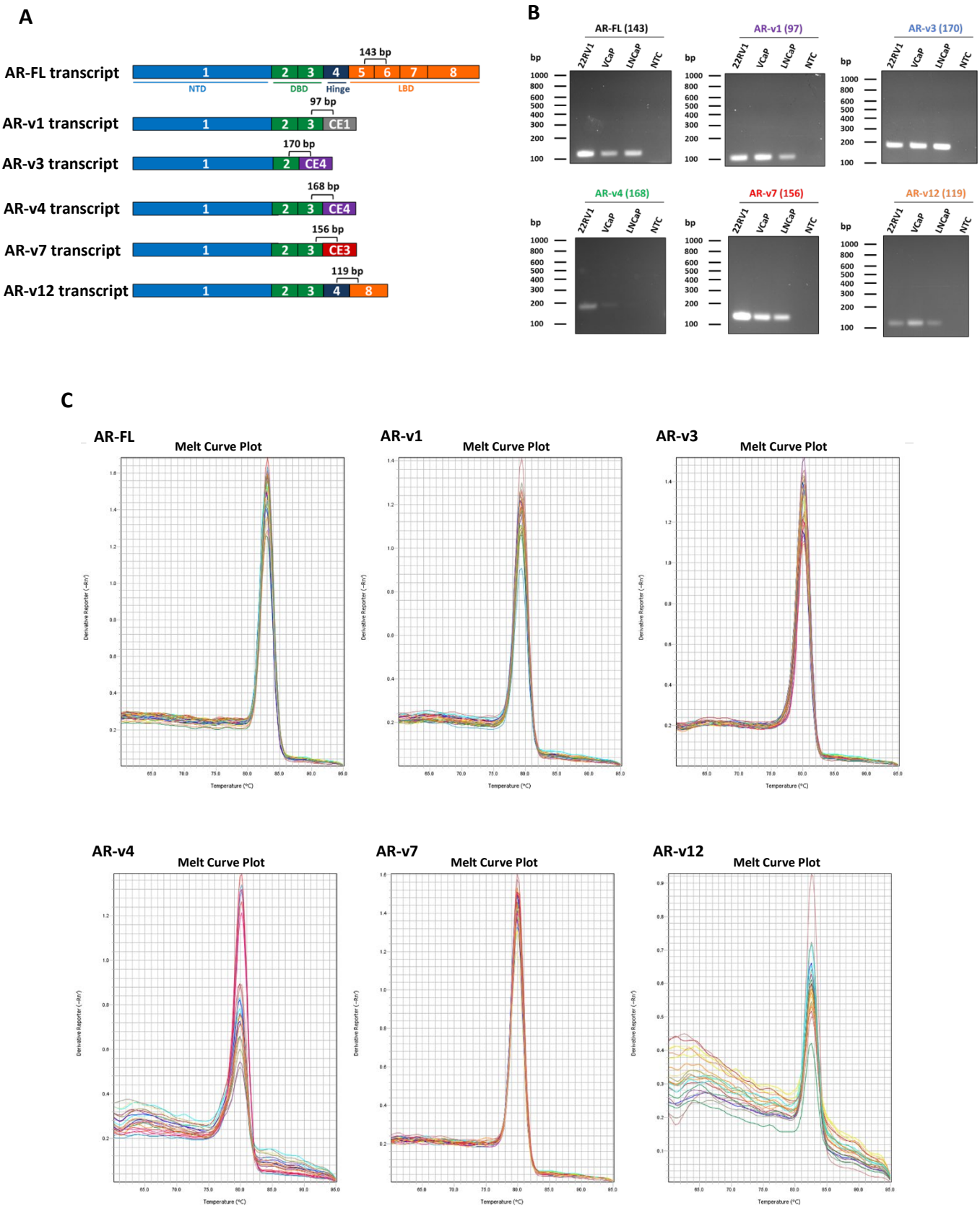

Supplementary Figure 3. AR-SV RT-PCR assay design and validation. (a) Based on previously described AR-SV sequences, transcript-specific primers were designed to anneal to unique sequences in each transcript to quantify specific AR transcripts using RT-PCR assays. Amplicon size is indicated. (b) PCR and agarose gel electrophoresis validation of AR isoform specific primers using AR-expressing PCa cell lines, 22RV1, VCaP and LNCaP, as positive controls compared to negative template controls (NTC). (c) Melt curves from each AR iso-form's RT-PCR amplification provide further evidence of each assay's specificity in human liver and prostate cells.

Supplementary figure 4

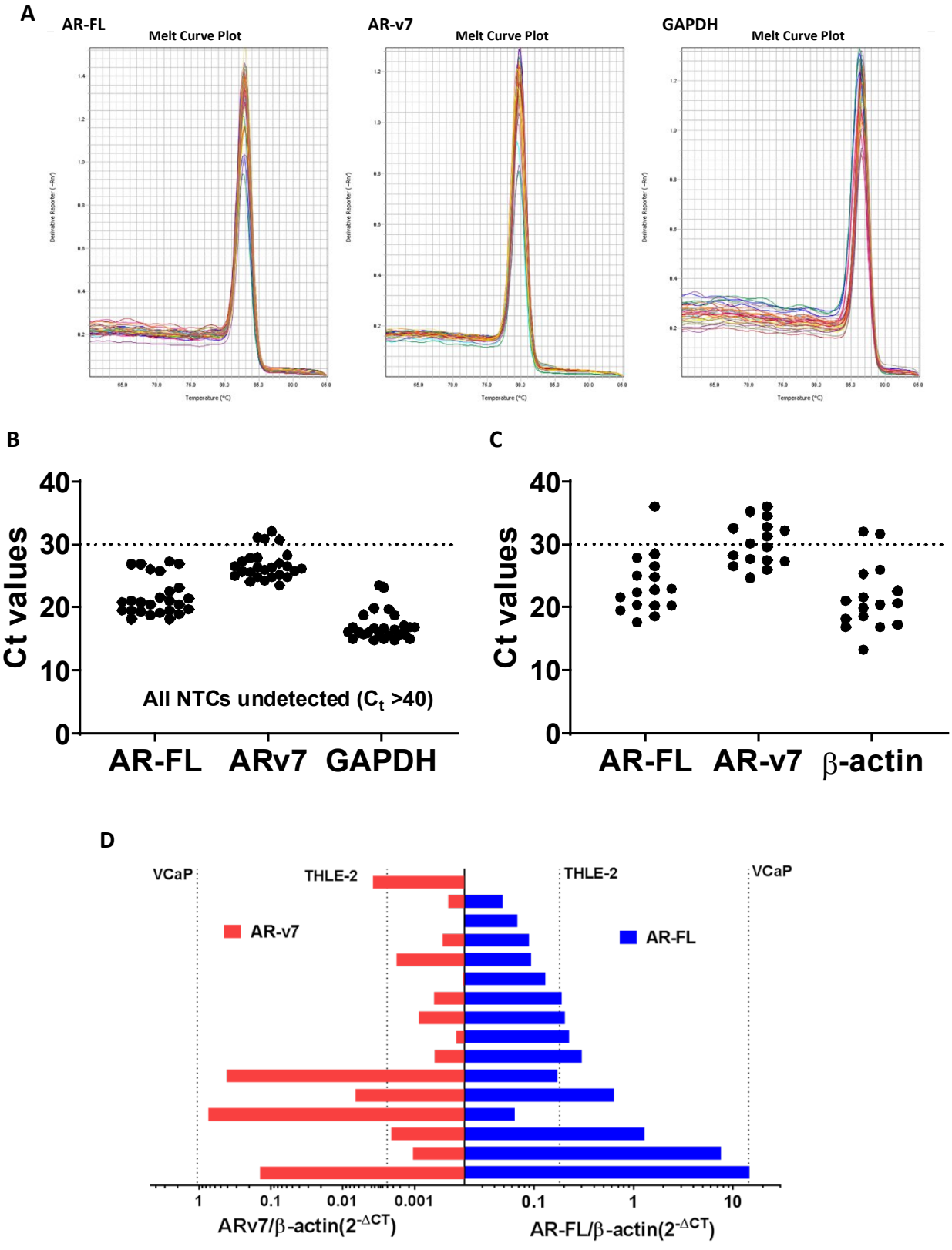

Supplementary Figure 4. Primary Tumor AR-v7 and AR-FL expression. (a) As in Supplementary Figure 3C, RT-PCR melt curves demonstrate assay specificity in primary HCC samples. (b, c) Representative plot of raw CT values to demonstrate robustness of AR isoform expression in patient samples from the James Cancer Center patients (b) and the National Liver Institute patients (c). (d) Analyses of tumor RNA from 16 HCC majority cirrhotic and chronic hepatitis infected patients who underwent liver resection (M=12, F=4). Levels are compared to negative control THLE-2 normal liver and positive control VCaP PCa cells to demonstrate abundant patient AR and AR-v7 expression. Bars represent average technical duplicates. Matched bars represent data from the same patient.

Supplementary figure 5

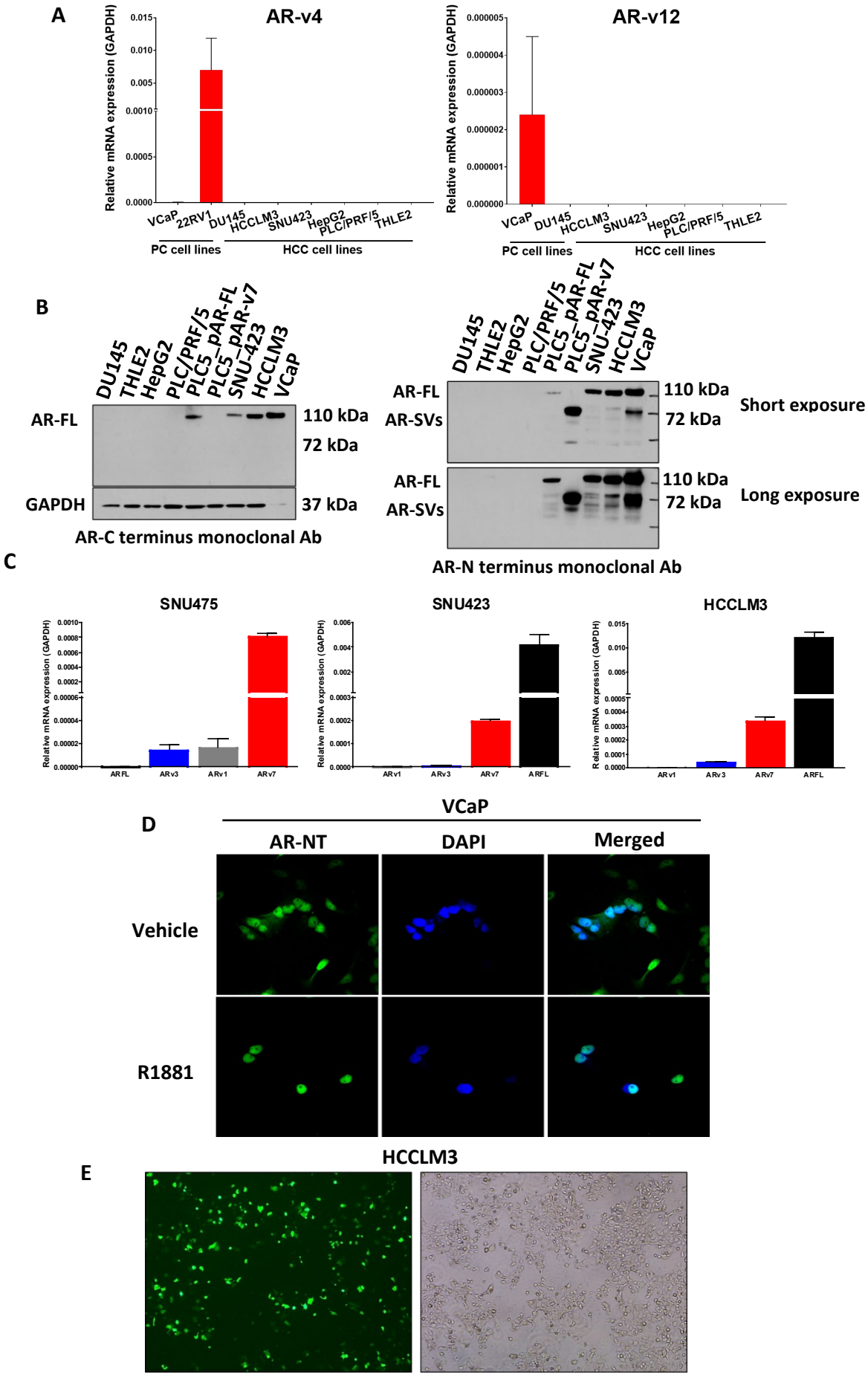

Supplemental Figure 5. Validation of C-terminal AR Western Blot using an N-terminal targeted mAb. (a) RT-PCR analyses of AR-v4 and AR-v12 transcripts in AR-positive prostate cancer (VCaP), AR-negative prostate cancer (DU145), AR-positive HCC (HCCLM3, SNU-423), AR-negative HCC (HepG2, PLC/PRF/5) and immortalized normal liver (THLE2) cell lines. (n=3, geometric mean ± SD). (b) To further confirm that the low molecular weight species that were detected by an N-terminal AR mAb are C-terminal truncated splice variants, the blot presented in Figure 1G performed with a C-terminal targeting AR mAb (blot from Figure 1G presented again here for convenience, *left*) was stripped, blocked and incubated with an N-terminal targeting AR mAb revealing abundant low molecular weight AR species (*right*). (c) RT-PCR analyses of low passage cells for AR-FL, AR-v1, AR-v3, and AR-v7 transcripts in AR-positive HCC (HCCLM3, SNU-423, SNU-475) from the Liver Panel ATCC Liver Cancer Panel TCP-1011 (n=3, geometric mean ± SD).(d) Immunofluorescence analysis of AR in VCaP performed using an N-terminal AR antibody as in (Figure 2B). Similar to HCCLM3 cells and irrespective of ligand, in VCaP N-terminal reactive AR species are predominately nuclear. (e) Transient transfection of a control GFP construct demonstrates the transfection efficiency of HCCLM3 using reagents as described in the materials and methods section.

Supplementary figure 6

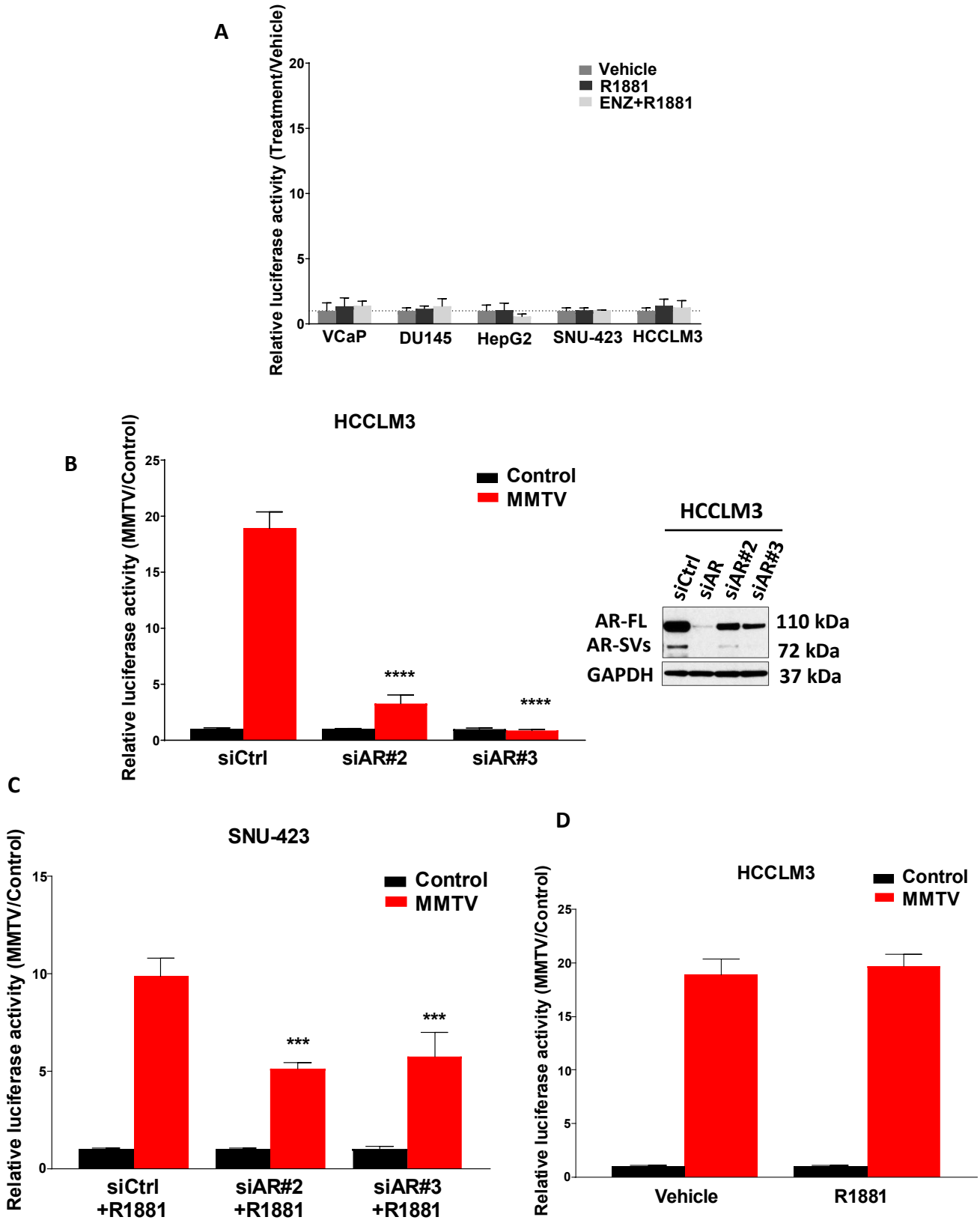

Supplemental Figure 6. AR transcriptional activity in HCC. (a) HCC (HepG2, SNU-423 and HCCLM3) and PCa (VCaP and DU145) cells were transiently transfected with basal promoter construct (pGL4.24-LUC) along with constitutively active renilla luciferase (RN-LUC) transfection control. Cells were maintained for 24 hours in charcoal-stripped FBS containing media (csFBS) then treated with vehicle, 1 nM R1881 or 10 μM enzalutamide (ENZ) with 1 nM R1881 for 24 hours. There was no significant transcriptional activation in cells relative to androgen-responsive construct (Figure 3A) indicating the promoter dependence of this effect. (b) Two additional siRNAs targeting AR were used to demonstrate the contribution of AR to the constitutive MMTV-LUC transcriptional signal in HCCLM3 cells using the dual luciferase assay as performed in Figure 3B. (c) In addition to the siRNA targeting AR shown in Figure 5F, two additional siRNAs targeting the AR were used to show that the MMTV-LUC signal resulting from 1 nM R1881 treatment in SNU-423 cells (as in Figure 3A) is AR-dependent. (d) Constitutive MMTV-LUC transcriptional activity in HCCLM3 cells (as determined in Figure 3B) was not able to be further stimulated following 24 hours 1 nM R1881 treatment. All panels: One-way ANOVA with Dunnett's multiple comparisons test. All panels: * $p<0.05$, ** $p<0.01$, *** $p<0.001$, and **** $p<0.0001$ versus siRNA controls.

Supplementary figure 7

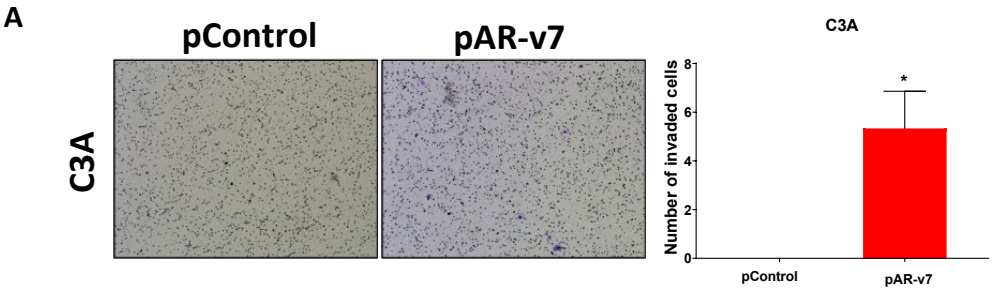

Supplemental Figure 7. AR transcriptional activity in HCC. (a) To determine the ability of AR-v7 to promote HCC cell invasion in an AR (-) HCC cell, HEPG2/C3A cells were transfected with an AR-v7 expression plasmid and expression vector control. Despite low innate invasive capacity, 48 hour cell invasion was slightly increased in AR-v7 expressing cells relative to controls. One-way ANOVA with Dunnett's multiple comparisons test. * $p<0.05$, ** $p<0.01$, *** $p<0.001$, and **** $p<0.0001$ versus expression plasmid controls.

Supplementary figure 8

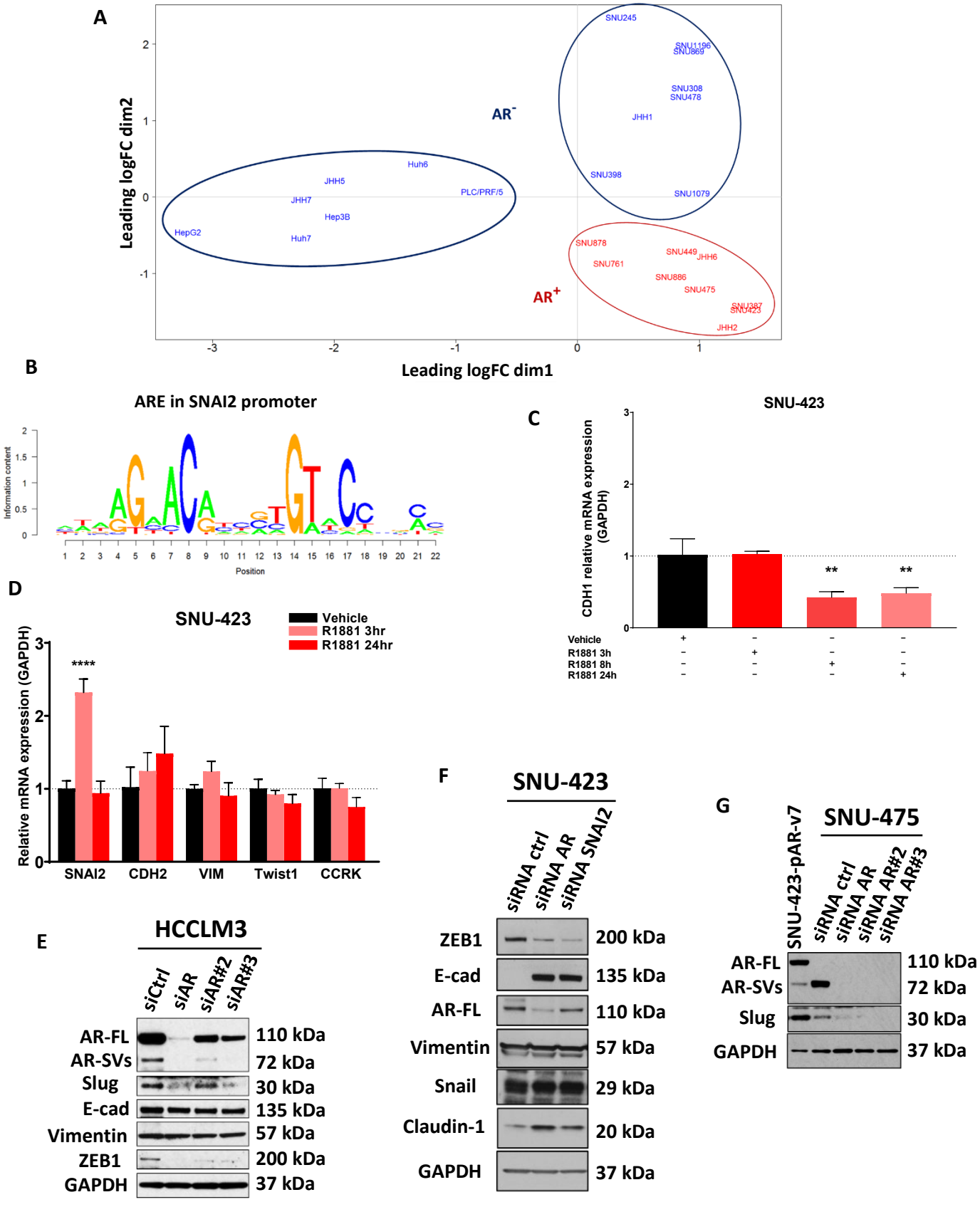

Supplementary figure 8. Differential gene expression analysis based on AR expression in HCC cell lines. (a) Multidimensional scaling plots for RNA-seq data of HCC cell lines from the CCLE. Using the previously described criteria (as noted in Figure 1C), each cell line was assigned to either an AR-negative group (*blue*) or an AR-positive group (*red*) then multidimensional scaling was performed using the edgeR package. This analysis demonstrates that AR-dependent transcriptomes can segregate AR-negative and AR-positive HCC cell lines. (b) A putative androgen response element (ARE) in the promoter region of SNAI2 was identified using MotifDb package in R identifying SNAI2 as a potential direct target of the AR. (c) RT-PCR shows that E-cadherin (downstream target of transcription repressor, slug) expression was decreased when SNU-423 cells were treated with 1 nM R1881 at 3, 8 and 24 hours relative to vehicle using one-way ANOVA with Dunnett's multiple comparisons test, **p<0.01 versus untreated control. (n=3, geometric mean ± SD). (d) Confirmatory RT-PCR shows that SNAI2 expression was increased when SNU-423 cells were treated with 1 nM R1881 at 3 hours relative to vehicle. Whereas no significant change in N-cadherin (CDH2), vimentin, twist-1 and cell cycle-related kinase (CCRK) expression were apparent. One-way ANOVA with Dunnett's multiple comparisons test was used, ****p<0.01 versus untreated control. (n=3, geometric mean ± SD). (e). Western blot analysis shows AR knockdown using two siRNAs for 24 hours, in addition to the siRNA experiment presented in Figure 3B, in HCCLM3 cells. AR knock down suppressed slug and ZEB1 protein expression. However, no change was observed in e-cadherin or vimentin levels. AR protein levels also presented in Supplementary Figure 6B (f) SNU-423 cells were transfected with either siRNA control, siRNA targeting AR or siRNA targeting SNAI2 in the presence of 1 nM R1881 (as in Figure

5F). ZEB1 expression was suppressed and E-cadherin expression induced with AR or SNAI2 knockdown. Claudin-1 levels increased following AR knock down with smaller changes resulting from SNAI2 silencing. No change in vimentin or snail protein expression resulted from either AR or SNAI2 knockdown. (g). WB analysis shows AR silencing using 3 different siRNA targeting AR in the AR-SV expressing HCC cell line SNU-475. Similar to findings in HCCLM3 and SNU-423 (Supplemental Figure 8E, F) AR knockdown results in suppression of slug protein.